



On the calculation of normalized viscous-plastic sea ice stresses

Jean-François Lemieux¹ and Frédéric Dupont²

¹Recherche en Prévision Numérique Environnementale/Environnement et Changement Climatique Canada, 2121 route Transcanadienne, Dorval, Qc, Canada.

²Service Météorologique Canadien, Environnement et Changement Climatique Canada, 2121 route Transcanadienne, Dorval, Qc, Canada.

Correspondence: J-F. Lemieux (jean-francois.lemieux@canada.ca)

Abstract. Calculating and plotting the normalized states of stress for viscous-plastic sea ice models is a common diagnostic for evaluating the numerical convergence and the physical consistency of a numerical solution. Researchers, however, usually do not explain how they calculate the normalized stresses. Here, we argue that care must be taken when calculating and plotting the normalized states of stress. A physically consistent and numerically converged solution should exhibit normalized stresses that are inside (viscous) or on (plastic) the yield curve. To do so, two possible mistakes need to be avoided. First, to assess the numerical convergence of a solution, one must compute the viscous coefficients and replacement pressure from the previous numerical iterate and the remaining strain rates from the latest iterate. Calculating the stresses only from the latest iterate falsely indicates that the solution has numerically converged. Second, the stresses should be normalized by the ice strength and not by the replacement pressure. Using the latter, one obtains converged states of stress that lie only on the yield curve (i.e., falsely indicating there are no viscous states of stress).

1 Introduction

Sea ice deformations, associated with the formation of leads, pressure ridges and shear lines, strongly influence the evolution of the sea ice cover in both polar oceans. As they affect the thickness distribution, sea ice deformations have an important impact on the exchange of heat, moisture and momentum between the atmosphere and the underlying ocean. To properly represent these processes in a model, it is essential that rheology, i.e. the relation between applied stresses, material properties and resulting deformations is correctly formulated.

Although some authors have recently proposed new sea ice rheologies (e.g., Girard et al. (2011)), most sea ice models are still based on the viscous-plastic (VP) formulation introduced by Hibler (1979). With the VP rheology, the ice is treated as a very viscous fluid (creep flow) when the internal stresses are small. However, once the stresses reach critical values defined by a yield curve, the ice flows as a plastic material and large deformations (i.e., spatial gradients of the velocity field) can occur.

When evaluating the physical consistency and numerical convergence of a VP solution, researchers often calculate and plot the normalized states of stress with respect to the yield curve. Unfortunately, they usually do not explain how they calculate this



25 diagnostic (e.g. Zhang and Hibler (1997); Hunke (2001); Lemieux and Tremblay (2009); Wang and Wang (2009); Kimmritz et al. (2015)). The purpose of this manuscript is to provide a short guide on how to calculate the normalized states of stress for assessing physical consistency and convergence of numerical solutions.

2 The viscous-plastic sea ice rheology

30 With the Hibler (1979) VP rheology, the components σ_{ij} of the stress tensor are given by

$$\sigma_{ij} = 2\eta\dot{\epsilon}_{ij} + [\zeta - \eta]\dot{\epsilon}_{kk}\delta_{ij} - P_p\delta_{ij}/2, \quad i, j = 1, 2, \quad (1)$$

where δ_{ij} is the Kronecker delta, $\dot{\epsilon}_{ij}$ are the strain rates defined by $\dot{\epsilon}_{11} = \frac{\partial u}{\partial x}$, $\dot{\epsilon}_{22} = \frac{\partial v}{\partial y}$ and $\dot{\epsilon}_{12} = \frac{1}{2}(\frac{\partial u}{\partial y} + \frac{\partial v}{\partial x})$ with u and v the components of the horizontal sea ice velocity vector, $\dot{\epsilon}_{kk} = \dot{\epsilon}_{11} + \dot{\epsilon}_{22}$, ζ is the bulk viscosity, η is the shear viscosity and P_p is the ice strength (we follow the notation of Kreyscher et al. (2000)).

35

The formulation of the viscosities depends on the yield curve and the flow rule. In the following, ζ and η are based on the widely used elliptical yield curve with a normal flow rule (Hibler, 1979):

$$\zeta = \frac{P_p}{2\Delta}, \quad (2)$$

$$\eta = \zeta e^{-2}, \quad (3)$$

40 where $\Delta = [(\dot{\epsilon}_{11}^2 + \dot{\epsilon}_{22}^2)(1 + e^{-2}) + 4e^{-2}\dot{\epsilon}_{12}^2 + 2\dot{\epsilon}_{11}\dot{\epsilon}_{22}(1 - e^{-2})]^{\frac{1}{2}}$, and e is the aspect ratio of the ellipse, i.e. the ratio of the long and short axes of the elliptical yield curve.

When Δ tends toward zero, equations (2) and (3) become singular. To avoid this problem, Hibler (1979) proposed to limit the maximum values of viscosities which is equivalent to limiting the minimum value of Δ . Hence, ζ is expressed as

$$45 \quad \zeta = \frac{P_p}{2\Delta^*}, \quad (4)$$

where $\Delta^* = \max(\Delta, \Delta_{min})$ with $\Delta_{min} = 2 \times 10^{-9} \text{ s}^{-1}$. Note that other approaches for limiting the viscous coefficients have been proposed (e.g., Kreyscher et al. (2000); Lemieux and Tremblay (2009)).

A drawback of the standard VP rheology is that the term $-P_p\delta_{ij}/2$ in equation (1) can cause the ice to deform even in the
 50 absence of forcing. To cure this problem, $-P_p\delta_{ij}/2$ is replaced by $-P\delta_{ij}/2$, where P is a function of the strain rates. The



simplest formulation of P is

$$P = P_p \frac{\Delta}{\Delta_*}, \quad (5)$$

where P tends toward zero for small deformations while it tends toward P_p for large deformations.

55

P is sometimes referred to as the replacement pressure (e.g., Hunke and Lipscomb (2010)). The use of a replacement method such as the one described above is now widely used in viscous-plastic sea ice models (e.g., Wang and Wang (2009); Losch et al. (2010); Hunke and Lipscomb (2010)).

60 3 Experimental setup

The divergence of the stress tensor (described in section 2), that is $\nabla \cdot \sigma$, is one of the terms of the sea ice momentum equation. The momentum equation is discretized in space and in time (see for example Lemieux et al. (2012) for details). It is either solved implicitly with a solver such as Picard (e.g. Zhang and Hibler (1997); Losch et al. (2010)) or with a Newton-like solver (e.g. Lemieux et al. (2012); Losch et al. (2014); Mehlmann and Richter (2017)) or it is solved explicitly with the elastic-VP
65 (EVP) approach (Hunke, 2001) or using the revised EVP with a pseudo-time stepping approach (e.g. Kimmritz et al. (2015)).

The numerical simulations for this paper were done with the Picard solver of the McGill sea ice model (see Lemieux and Tremblay (2009) for details). The spatial resolution is 10 km and the time step is 30 min. The model was restarted on January 1st 2002 12 UTC from a long-term simulation. The states of stress were calculated from solutions obtained at the first time
70 level (i.e., 12h30 UTC). We will discuss later how our conclusions apply to the other types of solvers.

With a Picard solver, one has to solve a nonlinear system of equations that can be concisely written as $\mathbf{A}(\mathbf{u})\mathbf{u} = \mathbf{b}(\mathbf{u})$ where \mathbf{u} is a vector that contains all the u and v velocity components on the grid, \mathbf{A} is a sparse matrix and \mathbf{b} is a vector that contains terms such as the atmospheric stress. It is important to mention that the elements of the matrix \mathbf{A} depend on the viscous
75 coefficients ζ and η and that the vector \mathbf{b} contains the replacement pressure P . The idea of implicit solvers such as Picard is to solve a series of linearized systems of equations in order to find the solution \mathbf{u} of the nonlinear system of equations. This algorithm can be expressed as

1. Start with an initial iterate \mathbf{u}^0

do $k = 1, k_{max}$

80 2. Solve $\mathbf{A}(\mathbf{u}^{k-1})\mathbf{u}^k = \mathbf{b}(\mathbf{u}^{k-1})$ with a linear solver

3. Stop if nonlinear convergence is reached



enddo

where the iterations of this loop are referred to as outer loop iterations (Lemieux and Tremblay, 2009).

85

It is crucial to note that when linearizing the system of equation (for step 2), ζ , η and P are expressed as a function of \mathbf{u}^{k-1} .

4 The calculation of normalized states of stress and results

We now discuss how the states of stress should be normalized and plotted in order to assess the physical consistency and the
 90 numerical convergence of the solution. We mean by physical consistency and numerical convergence that the states of stress
 are either inside (viscous) or on (plastic) the yield curve.

Using equation (1), equation (5) and the definition of Δ , one can obtain

$$P_p^2 \left(\frac{\Delta}{\Delta^*} \right)^2 = [\sigma_{11} + \sigma_{22} + P]^2 + e^2 [(\sigma_{11} - \sigma_{22})^2 + 4\sigma_{12}^2]. \quad (6)$$

95 Introducing the principal stresses σ_{p1} and σ_{p2} given by

$$\sigma_{p1}, \sigma_{p2} = \frac{\sigma_{11} + \sigma_{22}}{2} \pm \sqrt{\left(\frac{\sigma_{11} - \sigma_{22}}{2} \right)^2 + \sigma_{12}^2}, \quad (7)$$

equation (6) becomes

$$P_p^2 \left(\frac{\Delta}{\Delta^*} \right)^2 = [\sigma_{p1} + \sigma_{p2} + P]^2 + e^2 [(\sigma_{p1} - \sigma_{p2})^2]. \quad (8)$$

The correct way to normalize the stresses in equation (8) is to divide them by the ice strength P_p . Hence, we obtain

$$100 \left(\frac{\Delta}{\Delta^*} \right)^2 = \left[\frac{\sigma_{p1} + \sigma_{p2} + P}{P_p} \right]^2 + e^2 \left[\frac{\sigma_{p1} - \sigma_{p2}}{P_p} \right]^2. \quad (9)$$

With $\sigma_{p1}^n = \sigma_{p1}/P_p$ and $\sigma_{p2}^n = \sigma_{p2}/P_p$ we have

$$\left(\frac{\Delta}{\Delta^*} \right)^2 = \left[\sigma_{p1}^n + \sigma_{p2}^n + \frac{P}{P_p} \right]^2 + e^2 [\sigma_{p1}^n - \sigma_{p2}^n]^2. \quad (10)$$

Many authors (e.g., Zhang and Hibler (1997); Lemieux and Tremblay (2009)) have shown that an approximate solution that has not sufficiently converged exhibits unrealistic states of stress that are outside the yield curve. This is shown in Fig. 1. For



105 two (Fig. 1a) or 10 outer loop iterations (Fig. 1b), the solution has not converged and shows unrealistic states of stress. The fully converged solution (Fig. 1c) demonstrates physical consistency and numerical convergence. The fully converged solution was obtained by decreasing the L2-norm of the residual by a factor 1×10^{-8} . We also recommend the use of the residual for evaluating the numerical convergence of a solution as states of stress might be inside or on the yield curve even though the solution has not fully converged (Lemieux and Tremblay, 2009).

110

To obtain the results of Fig. 1 and therefore to be able to evaluate the numerical convergence of the solution, one has to consider the way the nonlinear system of equations is solved. Hence, the normalized principal stresses in equation (16) should be calculated from the linearized stresses expressed as

$$\sigma_{ij} = 2\eta(\mathbf{u}^{k-1})\dot{\epsilon}_{ij}(\mathbf{u}^k) + [\zeta(\mathbf{u}^{k-1}) - \eta(\mathbf{u}^{k-1})]\dot{\epsilon}_{kk}(\mathbf{u}^k)\delta_{ij} - P(\mathbf{u}^{k-1})\delta_{ij}/2. \quad (11)$$

115 In other words, the σ_{ij} should be calculated from viscous coefficients that are a function of the previous iterate \mathbf{u}^{k-1} and the strain rates from the latest iterate \mathbf{u}^k . These σ_{ij} are collocated at the tracer point of our C-grid. We now discuss two possible mistakes that could be done by modelers when assessing the physical consistency and numerical convergence of the solution.

120 First, let's consider that one calculates the stresses only based on the latest iterate \mathbf{u}^k , that is the viscous coefficients ζ and η and the replacement pressure are functions of \mathbf{u}^k instead of \mathbf{u}^{k-1} . Fig. 2 shows the normalized states of stress that are obtained in this case after only two outer loop iterations. One might conclude from this figure that the solution has converged as all the states of stress appear to be VP while we know this is not the case from Fig. 1a. This is important because a "true" converged solution exhibits better defined sea ice leads (and deformations, Lemieux and Tremblay (2009)), where large moisture/energy/salt fluxes are present between the sea ice, the ocean and the atmosphere.

125

This apparent numerical convergence of the solution is a consequence of the use of a rate-independent plastic rheology. This can be easily understood by considering a 1D viscous-plastic example. Assuming that sea ice does not have tensile strength and that it exhibits a large convergent deformation, the 1D relation between the stress (σ) and the deformation ($\dot{\epsilon} = \frac{\partial u}{\partial x}$) is given by

$$\sigma = \zeta\dot{\epsilon} - \frac{P}{2}, \quad (12)$$

130 where $\zeta = \frac{P_p}{2|\dot{\epsilon}|}$ and $P = P_p$ for a large plastic deformation.

Correctly expressing ζ as a function of \mathbf{u}^{k-1} and $\dot{\epsilon}$ as a function of \mathbf{u}^k , one obtains

$$\sigma = \frac{P_p}{2|\dot{\epsilon}^{k-1}|}\dot{\epsilon}^k - \frac{P_p}{2}, \quad (13)$$



which is equal to $-P_p$ only once the numerical solution has converged.

135

On the other hand, expressing both ζ and $\dot{\epsilon}$ as a function of \mathbf{u}^k leads to

$$\sigma = \frac{P_p}{2|\dot{\epsilon}^k|} \dot{\epsilon}^k - \frac{P_p}{2} = -P_p, \quad (14)$$

which is always equal to $-P_p$ whatever the velocity field \mathbf{u}^k used.

140 A second mistake that could be made by modelers would be to normalize the principal stresses with the replacement pressure P instead of using P_p . Hence, if we divide equation (8) by P^2 , we get

$$1 = \left[\frac{\sigma_{p1} + \sigma_{p2} + P}{P} \right]^2 + e^2 \left[\frac{\sigma_{p1} - \sigma_{p2}}{P} \right]^2. \quad (15)$$

With $\sigma_{p1}^n = \sigma_{p1}/P$ and $\sigma_{p2}^n = \sigma_{p2}/P$ we have

$$1 = [\sigma_{p1}^n + \sigma_{p2}^n + 1]^2 + e^2 [\sigma_{p1}^n - \sigma_{p2}^n]^2. \quad (16)$$

145 This is the equation of an ellipse we obtain if the principal stresses are normalized by the replacement pressure. The size and the center of the ellipse are therefore fixed. This is indeed what we obtain from a numerical experiment when we plot the stresses normalized by P . This is shown in Fig. 3 for two (a), 10 (b) and the fully converged solution (c). The normalized states of stress do not exhibit a realistic solution as all the stresses appear to be plastic. This is what explains the apparent absence of states of stress in the viscous regime in Fig. 18a and 18d of Wang and Wang (2009).

150

5 Conclusion

We have described how the normalized states of stress should be calculated and plotted in order to assess the numerical convergence and physical consistency of a VP solution. To do so, modelers should avoid two possible mistakes.

155 First, to evaluate the numerical convergence of an approximate solution, one should calculate stresses from viscous coefficients and replacement pressure that are a function of the previous iterate \mathbf{u}^{k-1} and the remaining strain rates from the latest iterate \mathbf{u}^k . This conclusion applies to all the implicit solvers. As the EVP and revised EVP approaches include time-stepping equations for the stresses, one simply needs to calculate the normalized stresses from the stress outputs. This issue of convergence is therefore more prone to occur with Picard and Newton-like solvers.

160



Second, the stresses should be normalized by the ice strength; not by the replacement pressure. Using the latter causes all the normalized stresses to lay on the yield curve, falsely indicating there are no stresses in the viscous regime. This issue can affect the implicit solvers but also the EVP and revised EVP approaches.

165 This manuscript should serve as a guide on how to calculate the normalized states of stress for assessing physical consistency and convergence of numerical solutions. It also complements and give more details about one of the sea ice diagnostics suggested for the CMIP6 sea-ice intercomparison project (Notz et al., 2016).

170 *Code availability.* The version (revision 333) of the McGill sea ice model used for the numerical experiments described in this manuscript is available on Zenodo at <http://doi.org/10.5281/zenodo.3530654>. The Zenodo deposit also includes the output files for the normalized stresses and the Matlab routine used for plotting.

Author contributions. JFL and FD derived the equations and designed the numerical experiments. JFL ran the experiments and wrote the manuscript.

Competing interests. JFL and FD do not have any competing interests.

175 *Acknowledgements.* We thank Amélie Bouchat and Bruno Tremblay for their helpful comments about this manuscript.



References

- Girard, L., Bouillon, S., Weiss, J., Amtrano, D., Fichefet, T., and Legat, V.: A new modeling framework for sea-ice mechanics based on elasto-brittle rheology, *Ann. Glaciol.*, 52, 123–132, 2011.
- 180 Hibler, W. D.: A dynamic thermodynamic sea ice model, *J. Phys. Oceanogr.*, 9, 815–846, 1979.
- Hunke, E. C.: Viscous-plastic sea ice dynamics with the EVP model: linearization issues, *J. Comput. Phys.*, 170, 18–38, 2001.
- Hunke, E. C. and Lipscomb, W. H.: CICE: the Los Alamos sea ice model documentation and software user’s manual version 4.1, Tech. Rep. LA-CC-06-012, Los Alamos National Laboratory, 2010.
- Kimmitz, M., Danilov, S., and Losch, M.: On the convergence of the modified Elastic-Viscous-Plastic method for solving the sea ice momentum equation, *J. Comput. Phys.*, 296, 90 – 100, <https://doi.org/https://doi.org/10.1016/j.jcp.2015.04.051>, <http://www.sciencedirect.com/science/article/pii/S0021999115003083>, 2015.
- 185 Kreyscher, M., Harder, M., Lemke, P., and Flato, G. M.: Results of the Sea Ice Model Intercomparison Project: Evaluation of sea ice rheology schemes for use in climate simulations, *J. Geophys. Res.*, 105, 11 299–11 320, 2000.
- Lemieux, J.-F. and Tremblay, B.: Numerical convergence of viscous-plastic sea ice models, *J. Geophys. Res.*, 114, C05 009, <https://doi.org/10.1029/2008JC005017>, 2009.
- 190 Lemieux, J.-F., Knoll, D. A., Tremblay, B., Holland, D. M., and Losch, M.: A comparison of the Jacobian-free Newton Krylov method and the EVP model for solving the sea ice momentum equation with a viscous-plastic formulation: a serial algorithm study, *J. Comput. Phys.*, 231, 5926–5944, <https://doi.org/10.1016/j.jcp.2012.05.024>, 2012.
- Losch, M., Menemenlis, D., Campin, J.-M., Heimbach, P., and Hill, C.: On the formulation of sea-ice models. Part 1: Effects of different solver implementations and parameterizations, *Ocean Model.*, 33, 129–144, <https://doi.org/10.1016/j.ocemod.2009.12.008>, 2010.
- 195 Losch, M., Fuchs, A., Lemieux, J.-F., and Vanselow, A.: A parallel Jacobian-free Newton-Krylov solver for a coupled sea ice-ocean model, *J. Comput. Phys.*, submitted, 2014.
- Mehmann, C. and Richter, T.: A modified global Newton solver for viscous-plastic sea ice models, *Ocean Modelling*, 116, 96 – 107, <https://doi.org/https://doi.org/10.1016/j.ocemod.2017.06.001>, <http://www.sciencedirect.com/science/article/pii/S1463500317300902>, 200
- 200 2017.
- Notz, D., Jahn, A., Holland, M., Hunke, E., Massonnet, F., Stroeve, J., Tremblay, B., and Vancoppenolle, M.: The CMIP6 Sea-Ice Model Intercomparison Project (SIMIP): understanding sea ice through climate-model simulations, *Geosci. Model Dev.*, 9, 3427–3446, <https://doi.org/https://doi.org/10.5194/gmd-9-3427-2016>, 2016.
- Wang, K. and Wang, C.: Modeling linear kinematic features in pack ice, *J. Geophys. Res.*, 114, C12 011, <https://doi.org/10.1029/2008JC005217>, 2009.
- 205 Zhang, J. and Hibler, W. D.: On an efficient numerical method for modeling sea ice dynamics, *J. Geophys. Res.*, 102, 8691–8702, 1997.

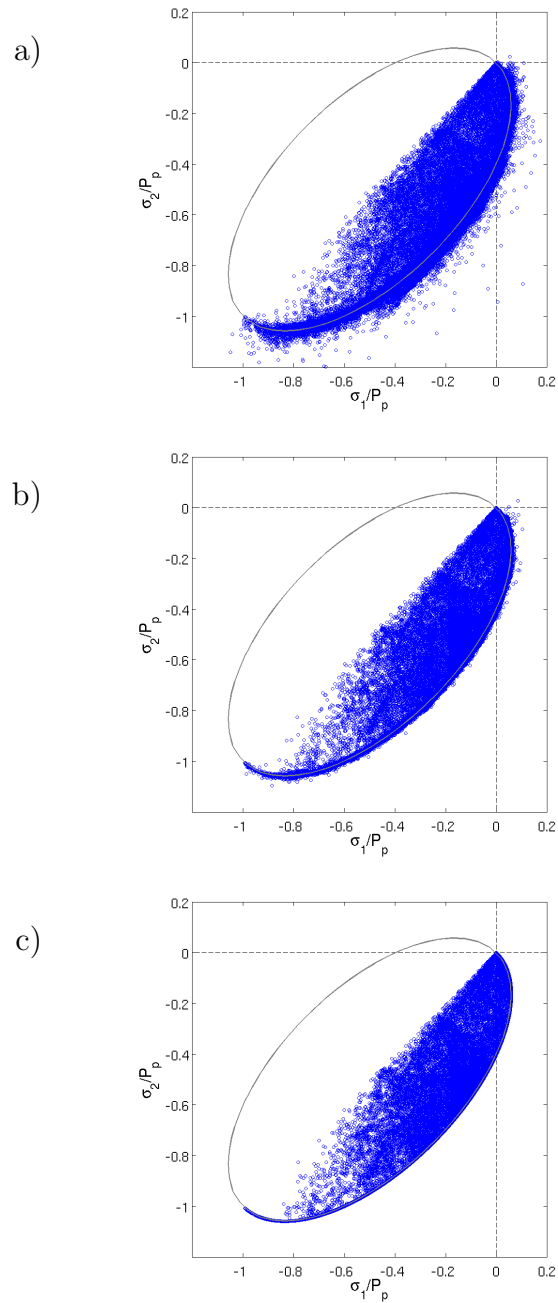


Figure 1. Principal stresses normalized by the ice strength P_p after two (a), 10 (b) outer loop iterations and the fully converged solution (c).

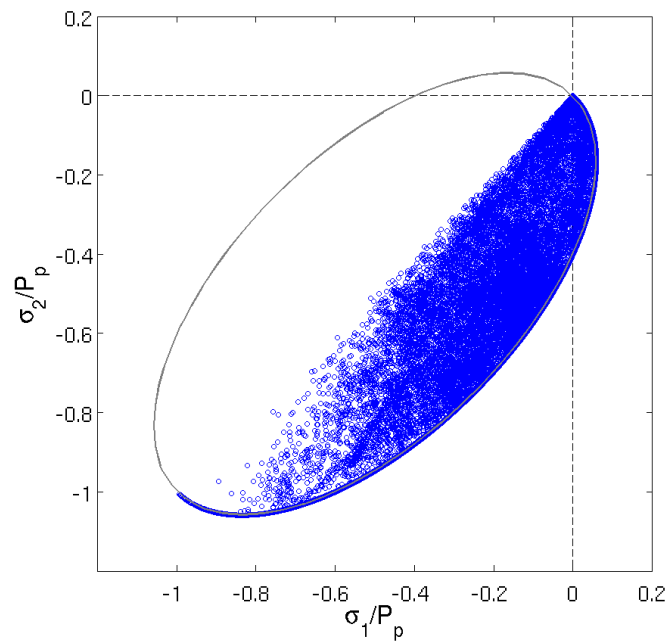


Figure 2. Principal stresses normalized by the ice strength P_p after two outer loop iterations. The solution appears to be numerically converged because the σ_{ij} are only a function of \mathbf{u}^k .

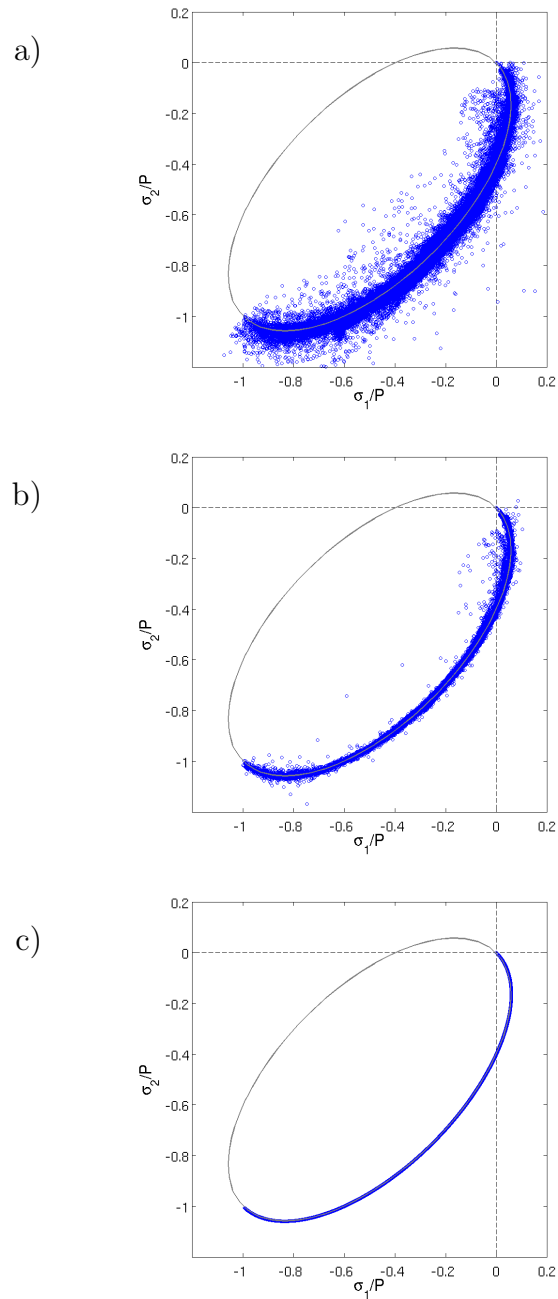


Figure 3. Principal stresses normalized by the replacement pressure P after two (a), 10 (b) outer loop iterations and the fully converged solution (c).